Experimental investigation into the effects of waves on blade loading for a model scale horizontal axis tidal turbine

Pragya Gupta, Malwattage Peiris, Jessica Walker, Sascha Kosleck and Irene Penesis

Abstract— **The effects of waves and turbine rotation on unsteady blade loads for an 800 mm diameter two-bladed model scale horizontal axis tidal turbine were investigated experimentally in a towing tank. This study presents data for four different scenarios, including a stationary or rotating turbine, different current velocities and different wave profiles. One of the rotor blades was instrumented with two strain gauges to measure the out-of-plane, M_y, and in-plane, M_x, blade root bending moments. The mean out-of-plane bending moment was approximately ten times larger than the in-plane bending moment. The mean bending moment coefficients, C_{My} and C_{Mx}, were not influenced by the presence of waves. However, wave-induced moments produced significant fluctuations of up to 27% and 78% for C_{My} and C_{Mx}, respectively, at the optimal tip speed ratio. Wave-induced and rotation-induced oscillations in the bending moments were clearly identified and for realistic operating conditions, the wave-induced oscillations dominated rotation-induced oscillations. The oscillations in M_y were in phase with the wave and drag dominated, whereas the oscillations in M_x were 180° out of phase with the wave and inertia dominated.**

Keywords—**Blade loads, blade root bending moment, marine current turbine, towing tank, waves.**

I. Introduction

TIDAL stream turbines are an emerging renewable energy technology, with the majority of currently installed devices being of the horizontal-axis type with 2 or 3 blades (e.g. MeyGen, Verdant, Sabella). Given the costs and risk associated with testing full-scale devices, developers and researchers typically use small model scale testing to assess new concepts and investigate device performance under various operating conditions [1].

Previous model scale experimental studies, e.g. [2]-[6], have found that the presence of waves can cause substantial fluctuations in the instantaneous power and thrust of horizontal axis tidal turbines, while mean values are largely unaffected. This has significant implications for power quality and structural loading, and hence material fatigue. It is vital that the unsteady loads on tidal turbines are understood to avoid additional maintenance or structural failure [2],[3] and enable accurate predictions of fatigue life and ultimate loads on turbine blades [7].

Lust et al [4] tested the same 800 mm diameter, 2 bladed rotor design as used in the present study in a 116 m long towing tank under the influence of both intermediate and deep water waves. They measured the torque and thrust of the rotor at various tip speed ratios and found that substantial fluctuations in power and thrust occurred with the passage of each wave. Similar results were found by Sos et al [5] for a smaller scale, 500 mm diameter turbine of the same design as [4], and Galloway et al [2] for a 3-bladed turbine. The oscillation in thrust and power will place additional strain on the turbine blades and increase fatigue loading [6].

The blade loads of interest are the out-of-plane (flapwise or axial), M_y, and in-plane (chordwise or radial), M_x, blade root bending moments. The coordinate system used in shown in Fig. 1. The rotor revolves about the x-axis, which is perpendicular to the plane of rotation. The z-axis is defined as the axis along the blade and the y-axis is in the plane of rotation, but perpendicular to the blades at any time as the coordinate system is blade fixed and hence rotates with the blade. The out-of-plane bending moment predominately results from the thrust forces on the blade and dominates the in-plane bending moment, which results from the gravitational and inertial forces [7].

There have been a limited number of studies that have experimentally measured the blade loads on tidal turbines, particularly under the influence of waves. Doman et al [1] measured blade loads on a 3-bladed 1/20th scale NREL S814 turbine rotor in a towing tank and presented a detailed uncertainty analysis but did not test under wave conditions. They determined axial and radial bending moment coefficients for a range of tow speeds and tip

Paper ID: 1470, Conference Track: Tidal Hydrodynamic Modelling

P. Gupta and M. Peiris were 4th year engineering students with the National Centre for Maritime Engineering and Hydrodynamics, Australian Maritime College, University of Tasmania, Launceston, Australia.

J. Walker and I.Penesis are with the National Centre for Maritime Engineering and Hydrodynamics, Australian Maritime College, University of Tasmania, Locked Bag 1395, Launceston, Tasmania, Australia, 7250 (email: Jessica.Walker@utas.edu.au, Irene.Penesis@utas.edu.au)

S. Kosleck is with the School of Engineering, Computer and Mathematical Sciences, Auckland University of Technology, Private Bag 92006, Auckland, New Zealand, 1142 (email: Sascha.Kosleck@aut.ac.nz)

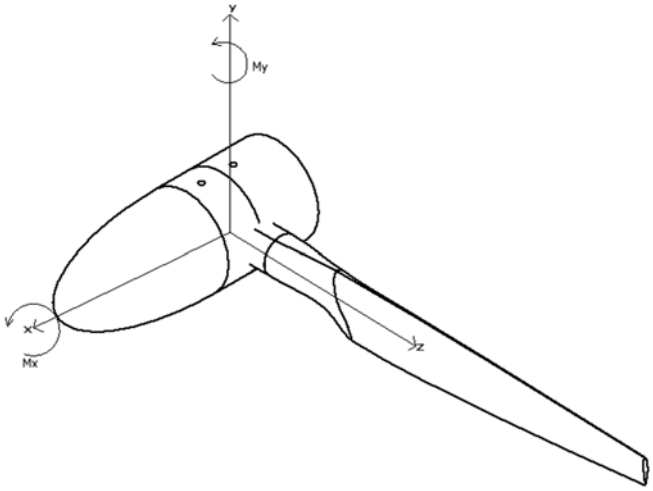

Fig. 1. Coordinate system and definition of blade root bending moments.

speed ratios, λ, and were able to show that both coefficients have an almost linear dependence on λ. Faudot and Dahlhaug [3] measured blade loads on a 2-bladed 1.475 m diameter rotor in a towing tank under several different wave states, primarily to validate numerical models.

Galloway et al [2] conducted experiments on a 1/20th scale 3-bladed turbine, including measuring the blade loads. They found that the maximum out-of-plane moment was up to 9.5 times the in-plane moment. Waves caused significant structural loading, with a loading range of 175% of the median out-of-plane moment and 100% of the median in-plane moment. Wave frequency was found to be more significant in terms of blade loading than the wave height.

Milne et al [7],[8] conducted experimental studies of a 780 mm diameter 3-bladed rotor in a towing tank, subjected to both steady and oscillatory (single and multifrequency) flow. The oscillations, designed to be similar to those caused by waves or turbulence, were induced using an auxiliary carriage system setup. The authors quantitatively assessed the role of unsteadiness on the blade root bending moment. Blade thrust and root bending moments were determined, but furthermore thrust and momentum coefficients for a variety of rotational periods were determined, showing that the magnitudes of wave induced force and momentum fluctuations are correlated to the rotational speed of the turbine. Their work clearly indicates that waves significantly contribute to the overall blade and total rotor loads.

Although model scale experiments deliver reliable results, their effectiveness with regards to examining wave induced loads is limited as wave encounter angles, other than head or following seas, are not considered, mainly due to limitations in the experimental setup. Numerical tools allow for more flexibility in the setup and methods like Computational Fluid Dynamics (CFD) can be used to investigate the effects of currents and superimposed waves on tidal turbines, including blade loads. However, these simulations are complex and time consuming.

Kosleck and Sprenger [9] numerically investigated wave induced effects on rotor blades for a revolving 3-bladed turbine for different combinations of wave period, rotor revolutions per minute (rpm) and wave encounter angle. Based on linear diffraction/radiation theory they were able to effectively identify wave induced blade forces and blade root moments covering a huge variety of incident waves from 0.01 to 2 rad/s and wave headings from 0 to 360°. Their approach allows, for a given rotor rpm, blade loads to be tracked as the rotor revolves. This generic and comprehensive approach enables a quick identification of worst-case scenarios from a huge variety of wave scenarios. The experimental data in the present study will be used to validate the numerical model in future planned work.

Previous studies of the model scale, 2-bladed horizontal axis tidal turbine design used in the present study focused on the performance of the turbine in terms of the power and thrust coefficient as a function of the tip speed ratio under different conditions including waves [4],[5], blade fouling [10], test facility and model scale [11]. This paper presents blade root bending moments for the turbine under the influence of waves based on a potential tidal turbine installation site in the Banks Strait, Australia. Mean and instantaneous data are analysed to determine the relationships between waves, currents, turbine rotation and blade root bending moments to better understand the loads on horizontal axis tidal turbine blades.

II. METHODOLOGY

The turbine rotor was tested in a 100 m long towing tank under four different scenarios, detailed in Section F, with waves of two different magnitudes, a stationary or rotating turbine and three different towing velocities. The following sections describe the turbine model, experimental setup, wave scaling, data acquisition and analysis, and finally a detailed description of each of the four test scenarios.

A. Physical Turbine Model

The two-bladed horizontal-axis turbine rotor model used is 800 mm in diameter and has a NACA 63-618 blade section with a blade twist of 13^{o} and a 62% taper. The rotor and hub are shown in Fig. 2. The rotor is a 1/25th scale model of a full-scale design by the United States National Renewable Energy Laboratory (NREL), similar in design to the decommissioned SeaGen turbine. The rotor has been extensively tested and the rotor blade geometry and performance curves (C_P and C_T versus λ) can be found in [4],[5][10],[11]. The rotor chord Reynolds number at 70% span, Re_{c70} varies from 1.6 x 10^5 (U = 1.25 m/s and λ = 4) to 6.2 x 10^5 (U = 2.25 m/s and λ = 9). The blade section used is Reynolds number independent at $Re_{c70} \geq 5 \times 10^5$ [10].

Fig. 2. Two-bladed turbine rotor and hub (800 mm diameter) with NACA 63-618 blades.

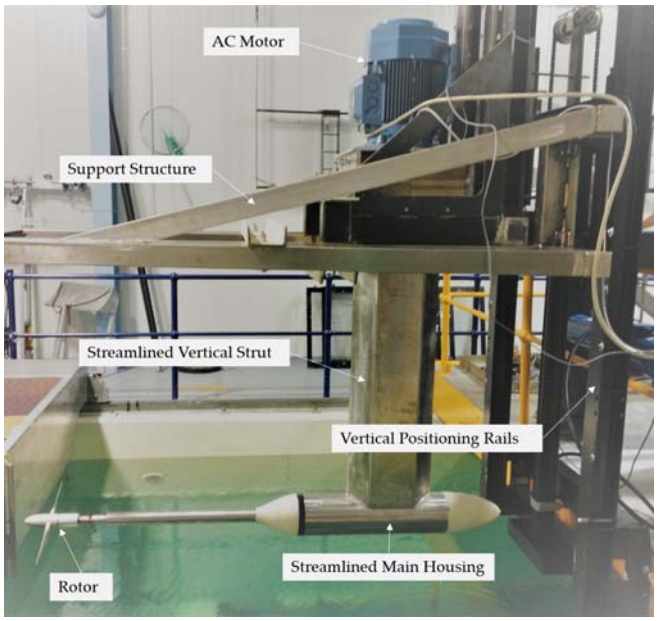

Fig. 3. Rotor installed on purpose-built test rig.

B. *Towing Tank and Instrumentation*

The turbine rotor was tested in the 100 m long towing tank at the Australian Maritime College, University of Tasmania, Launceston, Australia. The facility is 3.55 m wide and has a depth of 1.5 m. The turbine rotor was tested at towing speeds of 1.25 m/s and 2.25 m/s, similar to previous testing of the rotor in the same facility [5],[11]. A hydraulic wave maker is located at the end of the tank, capable of producing both regular and irregular waves.

The turbine rotor was installed on a purpose-built rig, shown in Fig. 4, with the hub located at a depth of 0.66 m. The rotor was driven by a vertically mounted AC motor and ABB variable frequency drive (VFD) controller, used to attain the required rotational speed and tip speed ratio. The axis of rotation was converted to the horizontal using a 90°, 1:1 gearbox, mounted in the main housing. An AMCI Dura Coder analogue encoder was attached to the gear box to track the blade position and rotational speed of the rotor.

One of the rotor blades was instrumented with two CEA-06-250UW-350 strain gauges to measure the blade root bending moments. The strain gauges were located on the cylindrical section of blade as close to the hub as possible, as shown in Fig. 4(a). The strain gauge cables were sent through the hollow shaft which was connected to a slip ring to transfer data from the strain gauges to the signal conditioner and amplifier. The strain gauges were calibrated according to International Towing Tank Conference (ITTC) procedures [12] by fixing the rotor to a

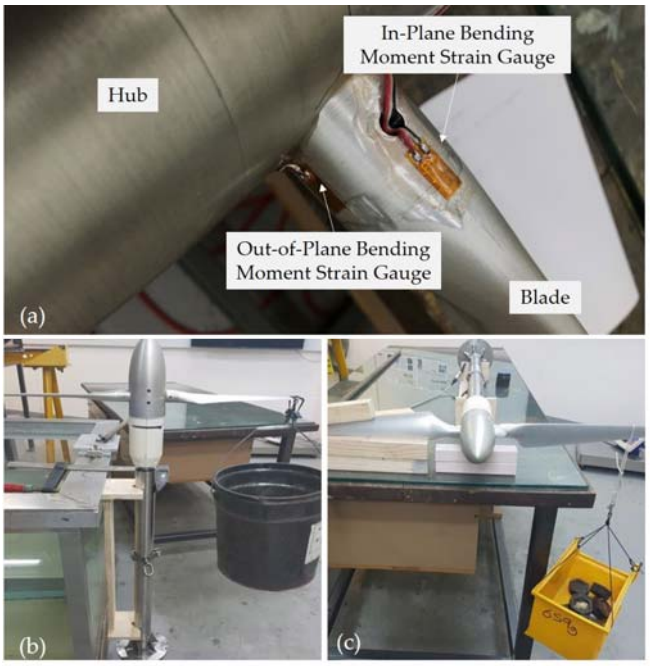

Fig. 4. (a) Strain gauges installed on rotor blade cylindrical section at the blade root, (b) Calibration of out-of-plane strain gauge, (c) Calibration of in-plane strain gauge.

workbench using wooden blocks and a G-clamp. A bucket was hung on the instrumented blade and weights incrementally added, as shown in Fig. 4(b and c).

Two wave probes were used in this experiment. The first was located near the wave maker to measure the incident waves. The second wave probe was fixed to the towing tank carriage, located approximately 200 mm downstream from the rotor plane and is travelling with the rotor at any given speed, revealing the waves as encountered by the rotor. The wave probes were calibrated daily during testing to maintain accurate readings in case of any changes in water level in the towing tank.

C. *Data Acquisition*

The towing tank carriage speed, shaft rotational speed from the analogue encoder, water surface elevations at the incident wave probe and carriage wave probe, and the out-of-plane and in-plane bending moments were measured at a sampling rate of 3 kHz. Zero values were obtained before each run with the carriage, rotor and water surface elevation stationary. The VFD was used to set the rotational speed of the rotor to achieve the desired λ. The wave maker was then started. The carriage was started when the waves were midway down the tank. The data was recorded for 30 seconds for tow speeds of 1.25 m/s, and 20 seconds for tow speeds of 2.25 m/s. Waiting periods of 20 to 30 minutes were set between each run to allow the water surface to fully settle, aided by retractable beaches along the length of the towing tank.

D. *Data Reduction and Uncertainty Analysis*

The performance of the rotor blades was evaluated using the non-dimensional tip speed ratio, λ, given in (1), out-of-plane bending moment coefficient, C_{My}, given in (2),

and in-plane bending moment coefficient, C_{Mx}, given in (3), where M_y and M_x are the out-of-plane and in-plane blade root bending moments, respectively, ρ is the water density, U is the current (towing) velocity, Ω is the rotational speed, R is the blade radius and A is the swept area of the rotor. The coordinate system used is given in Fig. 1.

$$\lambda = \frac{\Omega R}{U} \tag{1}$$

$$C_{My} = \frac{M_y}{\frac{1}{2}\rho U^2 A R} \tag{2}$$

$$C_{Mx} = \frac{M_x}{\frac{1}{2}\rho U^2 A R} \tag{3}$$

The calibrated data were filtered to remove noise and to isolate the cyclic effects of waves versus the rotation of the turbine. An example of the filtering applied is given in Fig. 5. Just the wave and out-of-plane bending moment data are shown in Fig. 5, however, the same filtering was applied to the in-plane bending moment. A slight offset can be seen between the wave signal and the out-of-plane bending moment signal in Fig. 5. This is, in part, caused by the wave probe being located approximately 200 mm downstream of the rotor plane due to setup constraints.

The filter was a bandwidth filter based on a Fourier Analysis of the raw data. A Fast Fourier Transform (FFT) algorithm was used to decompose the original signal into a number of harmonic components, resulting in a Fourier spectrum with a frequency-resolution of $d\omega=2\pi/\Delta T$, where ΔT is the duration of the measured signal. A lower as well as an upper frequency were defined to determine the frequency range to be kept. For all other frequencies the calculated Fourier coefficients were set to zero and the signal was subsequently re-assembled using an inverse Fast Fourier Transform (IFFT) applied to the modified spectrum. The bandwidth range was determined by test parameters such as wave period and rotational speed (rotational period), to make sure that wave- and rotation-induced effects remain visible.

For the results presented in this paper, wave data were filtered to only include frequencies in the range 0-6 rad/s. This range was determined by considering the wave encounter frequency seen by the turbine. The maximum wave encounter frequency of 5.41 rad/s occurs at a towing speed of 2.25 m/s for the minimum wave case which had an incident wave frequency of 0.5 Hz (π rad/s). The encounter frequency was calculated using (4), where ω_e is the wave encounter frequency in rad/s, μ is the wave heading (0 in this case) and ω is the incident wave frequency in rad/s. The effect of this filter can be seen in Fig. 5(a) which shows the unfiltered wave signal and

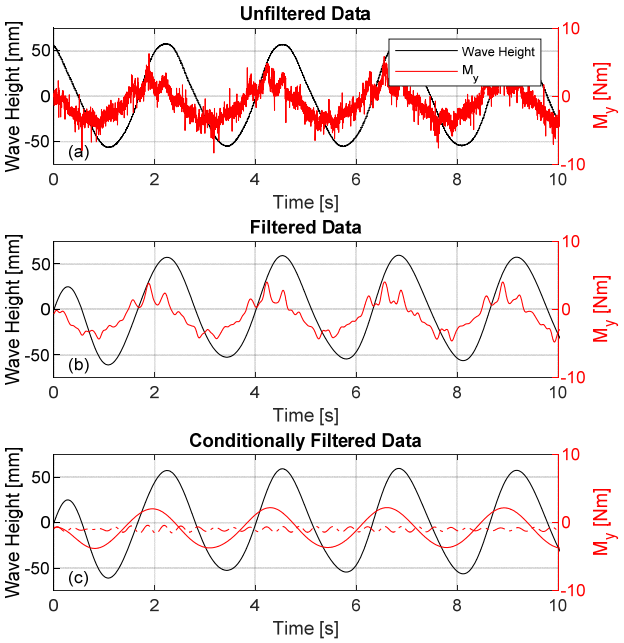

Fig. 5. Example filtering of wave and bending moment data. (a) Unfiltered data, (b) Filtered data: waves filtered for 0-6 rad/s, M_y filtered for 0-55 rad/s, (c) Conditionally filtered data: waves filtered for 0-6 rad/s, wave-induced M_y filtered for 0-6 rad/s (solid red line), rotation-induced M_y filtered for ± 2 rad/s of rotational frequency (dotted red line).

Fig. 5(b) and Fig. 5(c) which show the filtered wave signal, with high frequency noise removed.

$$\omega_e = \frac{U\omega^2}{g} cos\mu + \omega \tag{4}$$

The bending moment data (both out-of-plane and in-plane) were first filtered in the range of 0-55 rad/s. This range was determined by considering the expected range of turbine rotational frequencies. The maximum rotational speed tested was 483 rpm, corresponding to a rotational frequency of 50.7 rad/s, hence an upper cut-off of 55 rad/s was chosen. The effect of this filter can be seen by comparing the raw signal in Fig. 5(a) and the filtered signal in Fig. 5(b), with high frequency noise removed. The mean values presented in this paper represent 20 seconds of averaged data run through this filter.

To consider the effect of waves and turbine rotation separately, the bending moment data were also conditionally filtered, as shown in Fig. 5(c). To isolate the effect of waves, the data were filtered in the range 0-6 rad/s (solid red line in Fig. 5(c)). To isolate the effect of turbine rotation, the data were filtered in the range ± 2 rad/s of the rotational frequency of the turbine (dotted red line in Fig. 5(c)).

Previous studies of the same turbine in the same facility have reported a blockage ratio of 10% [11]. However, blockage corrections were not applied to the data, as there is not a blockage correction that can be applied to blade root bending moments [2].

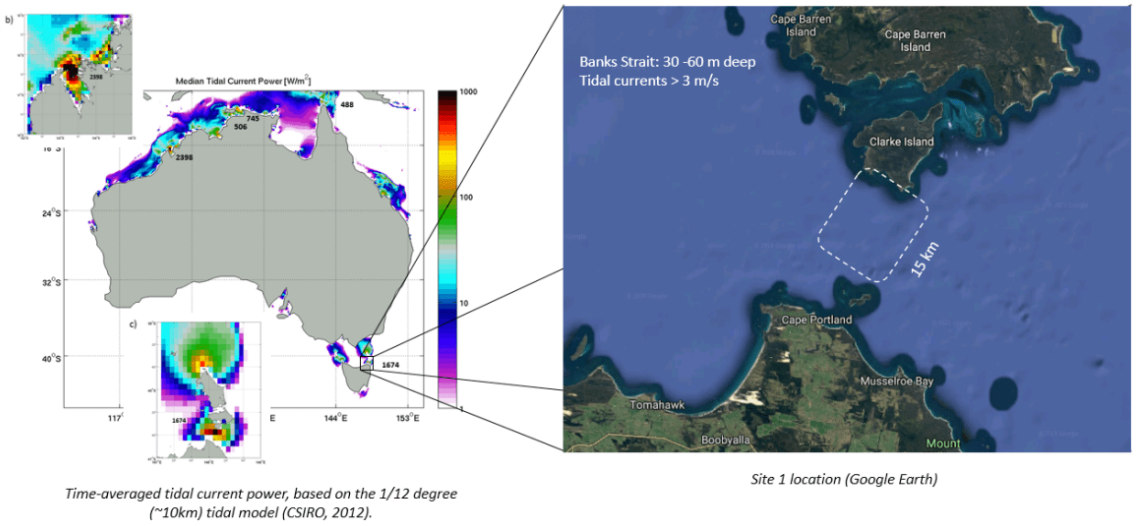

Fig. 6. Location of Banks Strait, Australia [14]

An uncertainty analysis was conducted according to the International Towing Tank Conference (ITTC) procedure [12] and [1]. The calibration, precision and bias errors were determined for each of the measured variables (carriage speed, rotational speed, out-of-plane and in-plane bending moment). The precision errors were determined by repeating a set of runs five times at $\lambda = 6$ with a wave height of 0.11 m and a towing speed of 2.25 m/s to determine the standard error in each measured variable. The precision error with a confidence interval of 95% was then calculated by multiplying the standard error of the parameter by the t-value from the t-distribution. The total errors, incorporating the calibration, bias and precision errors, in the out-of-plane and in-plane bending moments, M_y and M_x, were ± 7.3 % and ± 1.6 %, respectively.

E. *Wave Scaling*

The turbine rotor was tested under two different wave scenarios, based on the prevalent ocean conditions in the Banks Strait, Australia. The Banks Strait is a potential tidal energy installation site and is currently being mapped by the AUSTEn Tidal Energy in Australia Project [13]. The Banks Strait lies between the north-east tip of Tasmania and Clarke Island in the Furneaux Island group. The potential tidal energy site, shown in Fig. 6, is a 15 km wide channel with water depths of 25-60 m that are suitable for tidal turbine deployments. It has an estimated total tidal energy resource of 350 MW [14].

TABLE 1
FULL-SCALE WAVE DATA FOR THE BANKS STRAIT, AUSTRALIA

Wave Set	Wave Height H_s (m)	Wave Period T (s)	Wavelength L_w (m)	Steepness ratio H_s/L_w	Relative Depth h/L_w
Max	3	12.04	196	0.015	0.204
Min	1.5	10.50	157	0.009	0.255

TABLE 2
MODEL-SCALE WAVE DATA (SCALE 1/26.67)

Wave Set	Wave Height H_s (m)	Wave Period T (s)	Wavelength L_w (m)	Steepness ratio H_s/L_w	Relative Depth h/L_w
Max	0.11	2.34	7.35	0.015	0.204
Min	0.05	2.02	5.88	0.009	0.255

Full-scale wave data were extracted for the Banks Strait (Area 101) from the Global Waves Statistics database based on the two highest probability significant wave heights, given in Table 1. The full-scale data were scaled to model-scale values, given in Table 2, using the relative depth method described by Luznik et al. 2013 [15] where the steepness ratio, H_s/L_w, and relative depth, h/L_w, are kept constant, where H_s is the significant wave height, L_w is the wavelength and h is the water depth. The scaling was based on an average depth in the Banks Strait of h = 40 m and a towing tank depth of h = 1.50 m. Hence, the model scale for all test runs is 1/26.67. The experiments were run for both regular and irregular wave trains. Only the regular wave train results will be reported here.

F. *Test Scenarios*

Four overarching test scenarios were considered in this study, detailed in Table 3. The scenario with a stationary rotor, S1, provides the baseline loads on the rotor blades for the 'only waves' case. The turbine rotor was aligned in the upright position with the instrumented blade facing upwards.

Scenario R1 is not a realistic operating scenario but was run to determine the loads for a rotating turbine under the influence of waves with no current. Scenario R2 represents an operating turbine in the absence of waves, and R3 represents the worst-case scenario, an operating turbine in the presence of waves.

For the scenarios with a rotating turbine (R1, R2 and R3), tests were conducted for $4 < \lambda < 9$. For the scenarios with currents (R2 and R3), tests were run at towing speeds of 1.25 m/s and 2.25 m/s, similar to previous performance tests of the same rotor [5][11]. For scenarios with waves

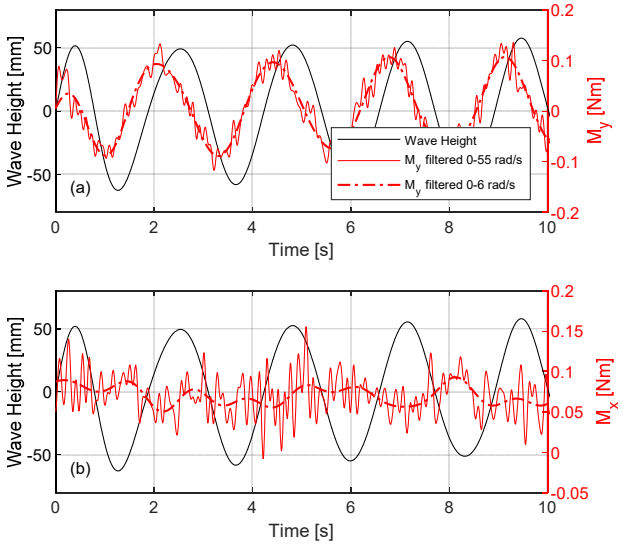

Fig. 7. Instantaneous wave and bending moment data for scenario S1 (stationary rotor with waves only), for the maximum wave case. (a) Out-of-plane moment, (b) In-plane moment.

(S1, R1 and R3), tests were run for both the maximum and minimum wave sets detailed in Table 2.

III. Results and Discussion

G. *Scenario S1: 'Stationary with waves only'*

The mean blade root bending moments for scenario S1 (stationary rotor with waves only) are given in Table 4. As expected, both the mean out-of-plane and in-plane bending moments are approximately zero, as the rotor is under the influence of waves only. The out-of-plane and in-plane bending moments fluctuate about the mean value by approximately ± 0.07 Nm and ± 0.08 Nm, respectively. The instantaneous data for the maximum wave set is shown in Fig. 7. The wave data were filtered for 0-6 rad/s. The bending moment data were passed through a general filter of 0-55 rad/s and a conditional filter to capture the wave-induced moments of 0-6 rad/s. Further detail on the filtering is given in Section D. The oscillation in the out-of-plane bending moment leads the wave by approximately 0.38 s. The carriage wave probe was offset behind the rotor plane by approximately 200 mm, giving an expected bending moment phase lead of 0.06 s. Thus, the bending moment phase lead cannot be entirely attributed to the experimental setup. The bending moment phase lead phenomenon was also reported by Milne et al [7] for low oscillation frequencies. The phase lead is discussed in further detail in Section J. The in-plane bending moment does not show a correlation with the wave phase. However, the asymmetry of the blade and its twist still lead to bending moments in the order of 25% of the out-of-plane bending moments.

TABLE 4
RESULTS FOR SCENARIO S1 ('STATIONARY WITH WAVES ONLY')

Wave Set	M_y (Nm)	M_x (Nm)
Max	0.008	0.053
Min	0.002	0.070

H. *Scenario R1: 'Rotating with waves only'*

The mean blade root bending moments as a function of turbine rotational velocity for Scenario R1 (rotating with waves only) are given in Fig. 8 for both the minimum and

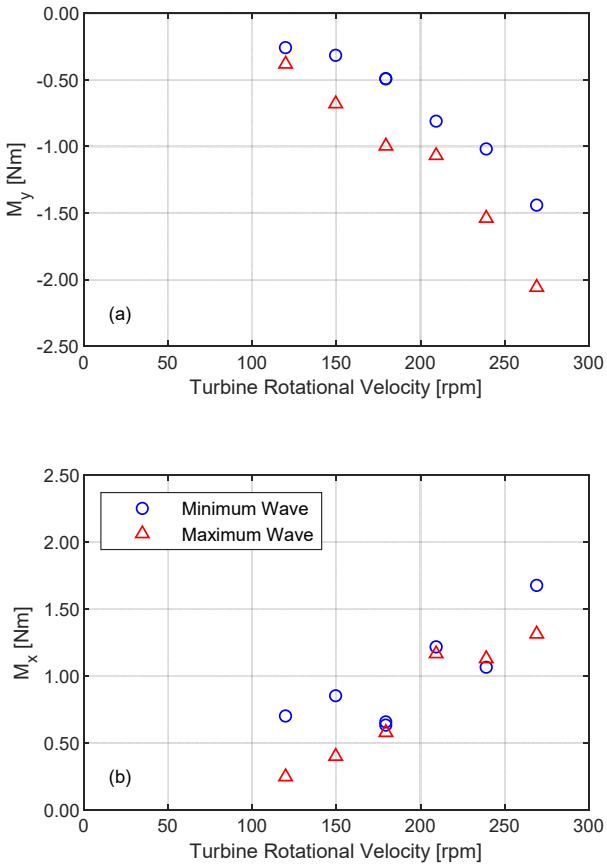

Fig. 8. Mean blade root bending moments for scenario R1 (rotating with waves only) at various turbine rotational velocities. (a) Out-of-plane moment, (b) In-plane moment.

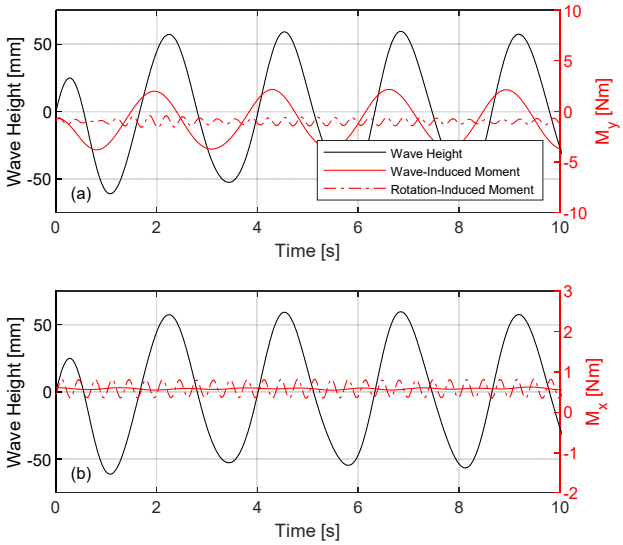

Fig. 9. Instantaneous, conditionally filtered wave and bending moment data for scenario R1 (rotating with waves only) for maximum wave case at a turbine rotational speed of 179 rpm. (a) Out-of-plane moment, (b) In-plane moment.

maximum wave cases. The absolute mean values of M_y and M_x are of the same order of magnitude for this scenario, whereas for scenarios with currents, mean values for M_y are significantly larger in magnitude than those for M_x.

The mean out-of-plane bending moment, M_y, is negative and its magnitude increases with increasing turbine rotational velocity (Fig. 8(a)). This is expected from blade element momentum theory, see [16]. The turbine was rotated with no currents ($U = 0$), hence $U_{rel} = \Omega r$, where U_{rel} is the relative velocity seen by the blade section and r is the local radius. The angle of attack, α, on the foil section is then negative and the relative wind angle is zero. For $\alpha < -4$ the lift coefficient, C_L, for the NACA 63-618 is negative. Thus, the thrust force on each blade is negative, resulting in a negative out-of-plane bending moment, as measured. The higher energy waves (maximum wave case) cause out-of-plane bending moments of larger absolute magnitude than the minimum wave case.

Considering the mean in-plane bending moment (Fig. 8(b)), M_x increases with increasing rotational velocity. The mean data are less conclusive regarding the effect of waves for this scenario.

Fig. 9 presents the instantaneous, conditionally filtered data for Scenario R1 at a turbine rotational speed of 179 rpm (corresponding to $\lambda = 6$, as if the turbine were towed at 1.25 m/s). Details on the filters applied are given in Section D. The out-of-plane bending moment, Fig. 9(a), is dominated by the waves, as the wave-induced moment is significantly larger than the rotation-induced moment (see Fig. 9(b)). Similar to Scenario S1, the oscillation in the wave-induced bending moment leads the wave phase by 0.23 s. The in-plane bending moment, Fig. 9(b), is dominated by the rotation of the turbine, and no wave-induced oscillation in M_x was observed. This was true for all rotational speeds tested.

I. Scenario R2: 'Rotating with currents only'

The mean blade root bending moment coefficients for scenario R2 (rotating with currents only) are presented as a function of the tip speed ratio in Fig. 10 and compared to predictions from blade element momentum (BEM) theory [16]. The experimental data for the two towing speeds show very good agreement up to $\lambda = 8$. There is a small separation between both the CM_y and CM_x values for the two towing speeds at $\lambda = 9$.

The out-of-plane bending moment coefficient, Fig. 10(a), increases with increasing tip speed ratio due to the increase in thrust (thrust coefficient curve available in [11]), consistent with [1], [2] and [7]. The in-plane bending moment coefficient, Fig. 10 (b), decreases in magnitude with increasing tip speed ratio, due to the reduction in rotor torque at higher λ [2].

The out-of-plane (flapwise) bending moment coefficient is approximately ten times larger than the absolute value of the in-plane (chordwise) bending moment coefficient. For example, at $\lambda = 6$, $C_{My} = 0.21$ and $C_{Mx} = -0.023$. This is consistent with the findings of Galloway et al [2] and Milne et al [7],[8].

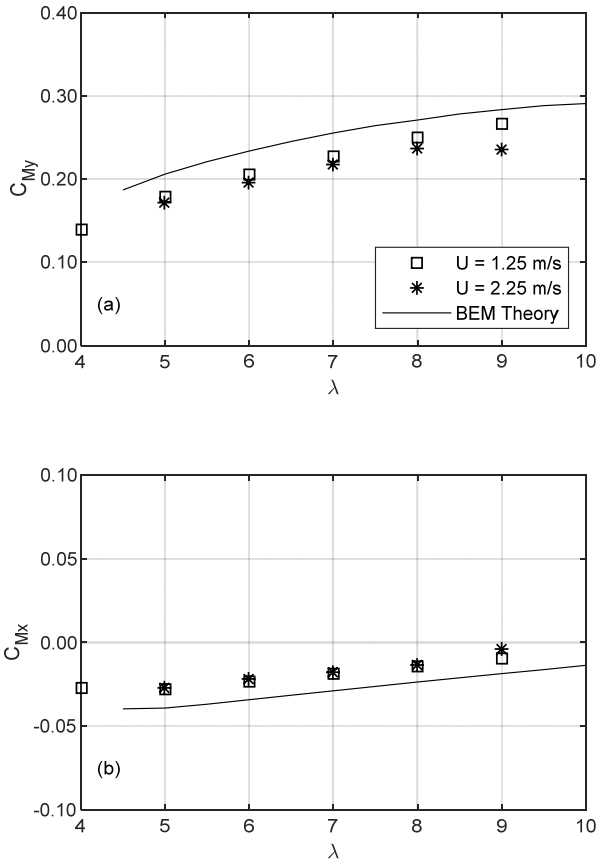

Fig. 10. Mean blade root bending moment coefficients for scenario R2 (rotating with currents only) compared to blade element momentum theory at various tip speed ratios. (a) Out-of-plane moment, (b) In-plane moment.

Results obtained by Walker et al [10] for a blade element momentum theory model of the same turbine are also presented in Fig. 10. The BEM power and thrust coefficients versus tip speed ratio curves were experimentally validated by [4] and [10]; the present study is the first study to examine the blade loads for the turbine model. The BEM curve for the out-of-plane bending moment follows the same trend as the experimental data but is on average 15% higher in magnitude. Similarly, the BEM curve for the in-plane bending moment follows the same trend as the experimental data but is on average 56% lower in magnitude (due to very small numbers involved).

J. Scenario R3: 'Rotating with currents and waves'

The mean blade root bending moment coefficients for scenario R3 (rotating with currents and waves) are presented as a function of tip speed ratio in Fig. 11 and compared to the data for scenario R2 (rotating with currents only). The presence of waves does not have an impact on the mean blade root bending moment coefficients. The data for no waves, minimum waves and maximum waves collapse onto the same curve for both the out-of-plane (Fig. 11(a)) and in-plane bending moments (Fig. 11(b)). This observation is supported by the findings of Galloway et al [2].

Conditionally filtered instantaneous wave and blade root bending moment coefficient data are presented in Fig. 12 for U = 2.25 m/s and λ = 6 for both the minimum (Fig. 12(a) and Fig. 12(b)) and maximum wave cases (Fig. 12(c) and Fig. 12(d)). Details on the filters applied are given in Section D. Similar trends were observed for the slower towing speed of 1.25 m/s. A tip speed ratio of λ = 6 was chosen as it is close to the optimal operating point for the turbine [10]. Similar trends were observed for the other tip speed ratios tested.

Considering Fig. 12, the change in magnitude of the rotation-induced bending moments (both out-of-plane and in-plane) depending on the wave case is insignificant. The wave-induced out-of-plane bending moment is in phase with the waves for both the minimum (Fig. 12(a)) and maximum (Fig. 12(c)) wave cases.

Conversely, the wave-induced in-plane bending moment is 180° out of phase with the waves for both the minimum (Fig. 12(b)) and maximum (Fig. 12(d)) wave cases. This is a very different response to that seen for Scenario R1 (rotating with waves only) for M_x, as can be seen by comparing Fig. 9b, where there was no wave-induced moment observed, and Fig. 12(b) or (d). Possibilities for this change in response include the change in wave encounter frequency and the tuning of the blade position with wave phase, which is discussed in more detail below.

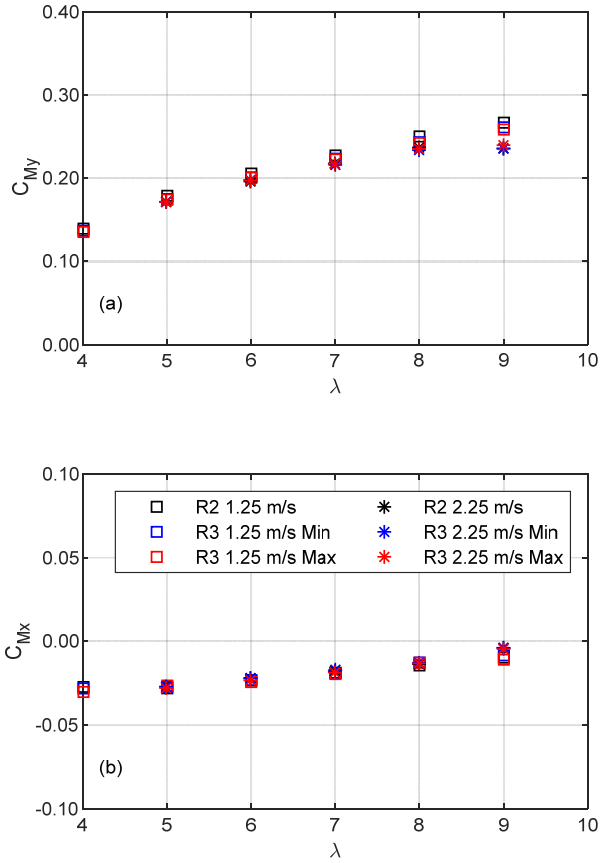

Fig. 11. Mean blade root bending moment coefficients for scenario R3 (rotating with currents and waves) compared to R2 (rotating with currents) at various tip speed ratios. (a) Out-of-plane moment, (b) In-plane moment.

The phenomena observed here for a rotating turbine in currents and waves are coherent with the theory as explained by the widely accepted Morison Equation. Considering that the shape of the blade is similar to that of a fixed cylinder, the Morison Equation interprets the total wave induced force by separating it into drag and inertia related components. The drag force component depends on the orbital water particle velocity underneath the wave, whereas the inertia component is caused by the water particle acceleration.

Considering the out-of-plane moment, M_y, it is obvious that this is predominantly caused by forces pointing in the x-direction, hence in the direction of wave travel. Forces in y- and z-directions can contribute to M_y as the blade is asymmetric about its longitudinal axis. However, these effects are marginal. The maximum and minimum horizontal water particle velocities u occur in phase with the wave (wave crest → u_{max}; wave trough → u_{min}), whereas

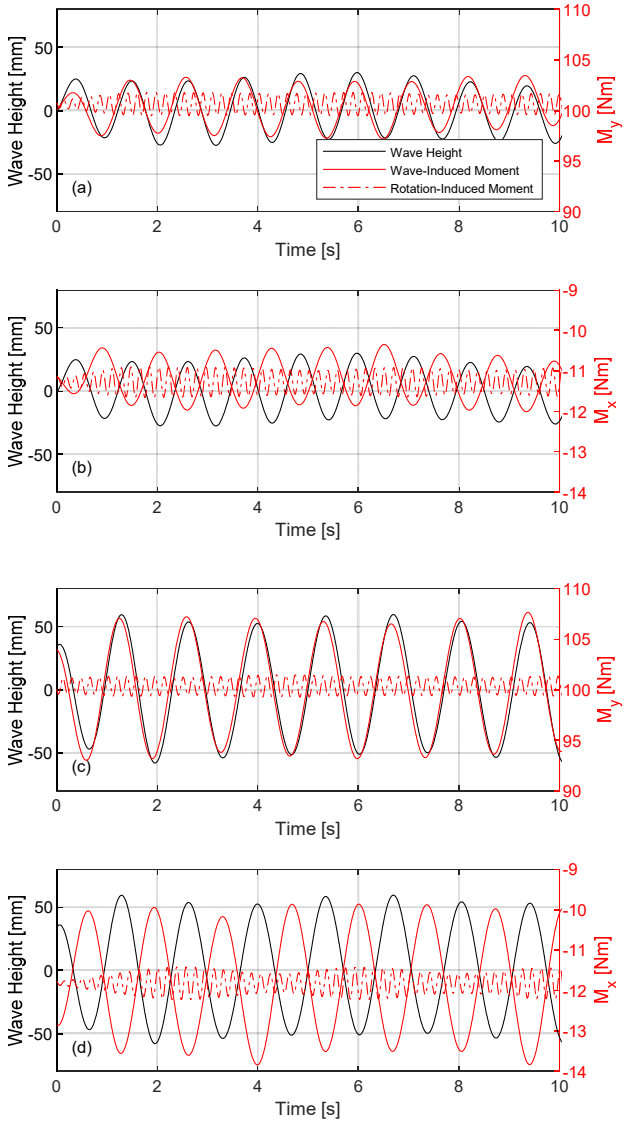

Fig. 12. Instantaneous, conditionally filtered wave and bending moment data for scenario R3 (rotating with currents and waves) at U = 2.25 m/s and λ = 6. (a) Out-of-plane moment, minimum wave case, (b) In-plane moment, minimum wave case, (c) Out-of-plane moment, maximum wave case, (d) Out-of-plane moment, maximum wave case.

the horizontal water particle acceleration leads with a phase shift of $\pi/2$ or 90° (wave zero-up-crossing → $\dot{u}_{max}$; wave zero-down-crossing → $\dot{u}_{min}$).

Hence, a moment dominated by the inertia force component would result in a phase shift by $\pi/2$. As Fig. 12 (a) and (c) display, this is not the case. Instead, the moment develops in phase with the wave and is therefore drag dominated. The actual position of the blade, as it revolves around the x-axis, should cause small fluctuations in the moment's magnitude as the magnitude of u and $\dot{u}$ decrease the further the blade is submerged into the water column.

For the in-plane moment, M_x, the situation is different. Considering the upright blade, obviously, forces in the x-direction cannot cause a moment M_x. Forces in the y-direction do result in a moment about the x-axis but, due to the experimental setup with all waves approaching perpendicular to the rotor plane, there are no velocities and accelerations in the y-direction. This leaves us with forces in the z-direction (vertical forces) as the main cause for any moment M_x measured. Clearly, with the blade being in an upright position, the moment a vertical force on the blade causes about the x-axis is comparatively small as its maximum lever is limited by the blade's dimension in the y-direction, hence the width of the blade.

With the blade pointing to the side, the situation changes significantly. Given the blade-fixed coordinate system, vertical forces, caused by vertical orbital water particle velocities and accelerations, are now acting in y-direction and therefore their lever on the blade can be as long as the length of the blade itself. Hence, in this position, the blade experiences a considerable moment M_x.

Again, using the Morison Equation, the total force can be separated into a drag and an inertia component, this time related to the vertical water particle velocity w and the vertical water particle acceleration $\dot{w}$, with w_{max} and w_{min} occurring during a wave zero-up-crossing and wave zero-down-crossing, respectively. Hence, drag forces caused by vertical water particle velocities are phase shifted by $-\pi/2$ with respect to the wave crest. Vertical water particle accelerations are, in relation to the velocities, again phase shifted by $-\pi/2$. Therefore, inertia forces are phase shifted in relation to the wave crest by $(-\pi/2-\pi/2) = \pi$ or 180°. As Fig. 12 shows a phase shift of 180° for M_x in relation to surface elevation, inertia forces dominate the in-plane moment.

In contrast to M_y, identifying the maximum possible in-plane moment for any given wave scenario is highly sensitive to the blade being "tuned" to the wave. That means that the maximum in-plane moment can be measured only if a wave crest/trough coincides with a sideways blade position. Any other combination does not reveal the maximum possible chordwise bending moments.

K. General Discussion

The mean bending moment coefficients for a given tip speed ratio were constant, regardless of the presence of waves. However, examining the instantaneous data, the bending moments fluctuate about the mean due to the presence of waves. A summary of the mean bending moment values and the fluctuations about the mean are given in Table 5 for a tip speed ratio of $\lambda = 6$ (or its equivalent rotational speed for the cases with no current) as an example. A tip speed ratio of $\lambda = 6$ is reported, as it corresponds to the maximum power coefficient for the turbine (see [10] or [11]). Given that C_{Mx} and C_{My} vary only on U and M_x and M_y, respectively, the percentage fluctuation in the bending moment coefficient is the same as the percentage fluctuation in the bending moment.

In the presence of currents only, at the optimal tip speed ratio of $\lambda = 6$, the out-of-plane and in-plane bending moments fluctuated by a maximum of 6% and 22%, respectively. In the presence of waves and currents the percentage fluctuation increased significantly, with the out-of-plane and in-plane bending moments fluctuating by a maximum of 27% and 78%, respectively, at the optimal tip speed ratio. The percentage fluctuation was higher for the maximum, more energetic wave case at the slower towing speed and increased with increasing tip speed ratio. At the highest tip speed ratio of $\lambda = 9$, the maximum increases encountered were 33% and 169% for

TABLE 5
BENDING MOMENT PARAMETERS FOR REPRESENTATIVE RUNS AT $\lambda = 6$ (OR EQUIVALENT) (FILTERED DATA)

Scenario	Towing Speed [m/s]	Rotor Speed [rpm]	Wave Case	$\overline{M_y}$ [Nm]	M_y Range [Nm]	M_y and C_{My} Range [%]	$\overline{M_x}$ [Nm]	M_x Range [Nm]	M_x and C_{Mx} Range [%]
S1	0	0	Min	0.002	-0.07 - 0.08	7714	0.05	-0.03 - 0.13	295
S1	0	0	Max	0.008	-0.12 - 0.15	3550	0.07	-0.02 - 0.16	244
R1	0	179	Min	-0.5	-2.4 - 1.8	860	0.6	0.4 - 1.0	105
R1	0	179	Max	-1.0	-5.3 - 4.2	950	0.6	0.3 – 0.9	108
R2	1.25	179	None	32.3	31.7 - 33.0	4	-3.7	-4.1 - (-3.3)	22
R2	2.25	322	None	99.7	97.2 - 103.2	6	-11.1	-12.2 - (-10.3)	16
R3	1.25	179	Min	31.5	29.4 - 33.9	14	-3.6	-4.4 - (-2.9)	42
R3	1.25	179	Max	31.5	27.3 - 35.8	27	-3.8	-5.4 - (-2.4)	78
R3	2.25	322	Min	100.6	95.2 - 104.7	9	-11.3	-12.6 - (-9.9)	24
R3	2.25	322	Max	100.3	91.3 - 108.3	17	-11.8	-14.6 - (-9.3)	44

the out-of-plane and in-plane bending moments, respectively. The loading ranges presented here are comparable to Milne et al [8] who reported increases of up to 15% for unsteady loads over the steady load case, but much smaller than those reported by [2], due to the different scaling effects [2].

IV. Conclusion

It is vital that the unsteady loads on tidal turbines are understood to avoid additional maintenance or structural failure [2]and enable accurate predictions of fatigue life and ultimate loads on turbine blades. The out-of-plane and in-plane blade root bending moments were measured on a model scale 2-bladed horizontal axis tidal turbine, which was tested under four different scenarios in a towing tank.

The following conclusions are drawn:

1) The presence of waves does not influence the mean blade root bending moment coefficients. However, wave-induced moments produce considerable fluctuations, which has implications for vibration and fatigue of the blades. The maximum fluctuations measured at the optimal tip speed ratio were 27% and 78% for the out-of-plane and in-plane bending moments, respectively.
2) The mean out-of-plane bending moment coefficient is approximately ten times larger than the absolute value of the in-plane bending moment coefficient.
3) The majority of the out-of-plane bending moment is current related.
4) Both wave-induced and rotation-induced bending moments can be clearly identified.
5) The out-of-plane bending moment, M_y, is in phase with the wave and is drag dominated.
6) The in-plane bending moment, M_x, is 180° out of phase with the wave and is inertia dominated.
7) For realistic cases, with currents, waves and rotation, the wave induced oscillations dominate rotation induced oscillations.

The Morison equation suggests that M_y will only have small fluctuations depending on blade position, whereas M_x is highly dependent on blade position in respect to the wave phase. This will be investigated in future work by further analysis of the experimental data to obtain the blade position in relation to wave phase. Future experimental work is recommended, including:

1) Tuning the blade position to the wave phase to examine the influence of blade position relative to the wave, particularly for the in-plane bending moment.
2) Extending the range of wave heights and frequencies tested.

Acknowledgement

The authors gratefully acknowledge the support of the Australian Maritime College Towing Tank technical staff, in particular Timothy Lilienthal and Kirk Meyer.

References

[1] D. Doman, R. Murray, M. Pegg, K. Gracie, C. Johnstone and T. Nevalainen, "Tow-tank testing of a 1/20th scale horizontal axis tidal turbine with uncertainty analysis," *International Journal of Marine Energy*, vol 11, pp. 105-119, 2015.

[2] P. Galloway, L. Myers, A. Bahaj, "Quantifying wave and yaw effects on a scale tidal stream turbine," *Renewable Energy*, vol 63, pp 297-307, 2014.

[3] C. Faudot, O. Dahlhaug, "Prediction of Wave Loads on Tidal Turbine Blades," *Energy Procedia*, vol 20, pp 116-133, 2012.

[4] E. Lust, L. Luznik, K. Flack, J. Walker and M. van Benthem, "The influence of surface gravity waves on marine current turbine performance," *International Journal of Marine Energy*, vol 3-4, pp. 27-40, 2013.

[5] M. Sos, L. Johnston, J. Walker and Rahimian, M, "The impact of waves and immersion depth on horizontal axis tidal turbine performance," in *12th European Wave and Tidal Energy Conference*, Cork, Ireland, 2017.

[6] N. Barltrop, K. Varyani, A. Grant, D. Clelland and X. Pham, "Investigation into wave-current interactions in marine current turbines," *Proc. Inst Mech Eng, Part A: J. Power and Energy*, vol 221, pp. 233-242, 2007.

[7] I. Milne, A. Day, R. Sharma and R. Flay, "Blade loads on tidal turbines in planar oscillatory flow," *Ocean Engineering*, vol 60, pp 163-174, 2013.

[8] I. Milne, A. Day, R, Sharma and R. Flay, "Blade loading on tidal turbines for uniform unsteady flow," *Renewable Energy*, vol 77, pp 338-350, 2015.

[9] S. Kosleck and F. Sprenger, "Maximum wave load cycles on submerged rotating tidal energy turbines – identification of worst case scenarios", in *Proceedings of AMSE 2017 36th International Conference on Ocean, Offshore and Artic Engineering*, Trondheim, Norway, 2017, vol 10.

[10] J. Walker, K. Flack, E. Lust, M. Schultz and L. Luznik, "Experimental and numerical studies of blade roughness and fouling on marine current turbine performance," *Renewable Energy*, vol 66, pp 257-267, 2014.

[11] M. Rahimian, J. Walker and I. Penesis, "Performance of a horizontal axis marine current turbine- A comprehensive evaluation using experimental, numerical and theoretical approaches," *Energy*, vol 148, pp 965-976, 2018.

[12] International Towing Tank Conference, "ITTC Quality System Manual Recommended Procedures and Guidelines, Uncertainty Analysis, Instrument Calibration", 2017. [Online] Available: https://www.ittc.info/media/7979/75-01-03-01.pdf

[13] AUSTEn Australian Tidal Energy Project, 2018. [Online] Available: www.austen.org.au

[14] AUSTEn Australian Tidal Energy Project, "Banks Strait field campaign kicks off", 2018. [Online] Available: www.austen.org.au/index.php/2018/03/17/banks-strait-field-campaign-kicks-off/

[15] L. Luznik, K. Flack, E. Lust and K. Taylor, "The effect of surface waves on the performance characteristics of a model tidal turbine," *Renewable Energy*, vol 58, pp 108-114, 2013.

[16] J. Manwell, J. McGowan, A. Rogers, "Aerodynamics of Wind Turbines," in *Wind Energy Explained Theory, Design and Application*, 2nd ed. John Wiley & Sons, 2009, ch. 3, pp 117-121.